IN-46
151051
P.31

NASA Contractor Report 4498

Inner Magnetosphere Imager (IMI) Instrument Heritage

G. R. Wilson

GRANT NGT-01-002-099
MARCH 1993

(NASA-CR-4498) INNER MAGNETOSPHERE IMAGER (IMI) INSTRUMENT HERITAGE (Alabama Univ.) 31 p

N93-22685

Unclas

H1/46 0151051

NASA Contractor Report 4498

Inner Magnetosphere Imager (IMI) Instrument Heritage

G. R. Wilson
The University of Alabama in Huntsville
Huntsville, Alabama

Prepared for
George C. Marshall Space Flight Center
under Grant NGT-01-002-099

National Aeronautics and
Space Administration

Office of Management

Scientific and Technical
Information Program

1993

TABLE OF CONTENTS

ii INTENTIONALLY BLANK

PRECEDING PAGE BLANK NOT FILMED

LIST OF ILLUSTRATIONS

CONTRACTOR REPORT

INNER MAGNETOSPHERE IMAGER (IMI) INSTRUMENT HERITAGE

INTRODUCTION

This document contains heritage information for the list of instruments, generated by the Inner Magnetosphere Imager (IMI) science working group, for the proposed IMI spacecraft [Herrmann, 1992]. As one might imagine, the heritage situation for these instruments is very uneven. Some of them have so much heritage that it is conceivable that when IMI is being built, off the shelf instruments could be used. Others have so little heritage that it is not even clear that there exists a signal to measure. The Auroral Imager (FUV) and the Geocoronal Imager both have direct heritage. Many instruments designed to image the aurora (at visible and ultraviolet wavelengths) and the geocorona (at 1,216 Å) have been built, flown, and successfully operated. These instruments have improved over the years so that it appears that there will be little difficulty in meeting the IMI requirements for these instruments. The proton and electron precipitation imagers have a more limited background in that instruments have been designed to perform these functions, but their use or their capabilities are significantly different from those required for IMI. The He^+ 304 Å camera has no direct instrument heritage but does have a great deal of technological heritage. The O^+ 834 Å camera has the least heritage of any instrument. The technology that could be used for this camera is still mostly in the conceptual stage. The amount of magnetospheric production of 834 Å radiation is highly uncertain, and it appears that the flux may be too weak to measure.

In the next 2 years, a number of instruments which will test magnetospheric imaging will be flown. These include an ultraviolet (UV) auroral imager (UVI), a visible auroral imager (VIS), an electron precipitation imager (PIXIE), and an instrument with neutral particle imaging capabilities (SEPS), all of which will be carried on the ISTP Polar (launch in June 1993?) spacecraft's despun platform. In the fall of 1992, a He^+ 304 Å plasmaspheric imager called WIDGET will be launched on a sounding rocket to test its capabilities. An energetic neutral atom imager called ISENA is scheduled for a mid-1994 Pegasus launch on the SAC-B satellite. The JASPR instrument, designed to image proton aurora on Jupiter, will be reflown in June 1993, and hopefully will be able to acquire its target. It would be very helpful for IMI planning to keep tabs on these flights to see how well these instruments work.

AURORAL IMAGERS

The following discussion describes eight different types of auroral imaging instruments which have been used over the last 20 years. This list is not complete, but is extensive enough to cover most of the efforts in this field. There is no effort made here to discuss the work done via spacecraft or sounding rocket, to observe, but not directly image, optical and UV auroral emissions by photometers or spectrometers. These measurements can be used to do a crude form of auroral imaging since instrument output as a function of spacecraft attitude or location are often obtained. (See Chubb and Hicks, 1970, for an example of this.) This type of imaging, though, is obviously not in the vein of what is being considered for IMI. There are also no remarks here about ground-based auroral imaging with all-sky cameras. Global images of the aurora can only be obtained from the ground with a network of cameras, but because of atmospheric absorption of auroral UV, this work is restricted to the visible portion of the spectrum.

Imaging of the aurora by spacecraft has been carried out for over 20 years. The first imagers were flown on Air Force weather service satellites (DMSP), starting in the early 1970's [Rodgers, 1974]. These spacecraft were placed in highly inclined, nearly circular orbits at altitudes near 850 km. The instrument that imaged the aurora was a line scanning radiometer that used a broad filter whose response peaked at 8,000 Å. It integrated several important auroral emissions in the visible portion of the spectrum at 6,300 Å, 6,364 Å, 5,577 Å, and band emissions from N_2 and N_2^+. The instrument scanned its field-of-view in the direction perpendicular to the spacecraft velocity vector by means of a mirror rotating at 1.78 revolutions per second (r/s). Each mirror revolution produced an image strip 3.7 km by 3,000 km on the Earth's surface. A two-dimensional image was formed by successive scans made along the spacecraft ground track. This instrument was not able to image the whole aurora on a single orbital pass.

In 1973, the ISIS-II spacecraft carrying a scanning auroral photometer [Anger, 1973] was launched into a circular polar orbit at 1,400-km altitude. This auroral imager consisted of two imaging heads with a single common detector. Each head had a narrow pass band transmission filter; one at 5,581 Å and the other at 3,915 Å. A full image was built up from successive scans made by each revolution of the spacecraft (3 r/min). Each scan strip had a ground length of 4,000 km. The 5° field-of-view perpendicular to the spin scan direction was divided into thirteen 0.4° bins and electronically scanned on a fast time scale. The angular resolution of the imager was 0.4° by 0.4°.

The Japanese launched a satellite for studying the aurora (named Kyokko, which means aurora in Japanese) into an orbit inclined at 65° with an apogee of 3,974 km, on February 4, 1978 [Hirao and Itoh, 1978]. This satellite carried a UV auroral television camera (ATV) which consisted of an image-memory tube outfitted with a MgF_2 window and a KBr photocathode [Frank et al., 1981]. This combination made the instrument sensitive to the vacuum ultraviolet between 1,200 and 1,400 Å. Thus, it viewed the auroral emissions from atomic hydrogen at 1,216 Å, atomic oxygen at 1,304 and 1,356 Å, and the short wavelength end of the LBH bands of N_2. The viewing optics had an angular resolution of 0.3° in a full field-of-view of 60°. The image repetition rate was 2 min, although it is not clear that this capability was used to do time evolution studies of the aurora, possibly because of limited tracking coverage or spacecraft memory.

The DE 1 spacecraft, launched in 1981, carried a sophisticated imaging system (SAI) designed to perform a number of imaging tasks [Frank et al., 1981]. This instrument consisted of three separate assemblies, each with its own optical system, filters (12), and a photomultiplier tube (fig. 1). Two of the assemblies were optimized, by choice of the photocathode material and the filters, for imaging in the visible portion of the spectrum (3,175 to 6,300 Å), while the third was designed for the vacuum ultraviolet (1,200 to 1,800 Å). Each imaging assembly had a small, instantaneous field-of-view of about 0.3° which resulted from a long entrance collimator, an off-axis focusing mirror, and a pinhole placed before the filter. This arrangement was needed in order to eliminate stray light. A two-dimensional image was built up by scanning in one direction by spacecraft roll (spin rate—10 r/min) and in the perpendicular direction by a stepping mirror. The stepping mirror advanced 0.25° every spacecraft revolution. Since successive pixels were overlapped in both directions, the instrument angular resolution was 0.25° by 0.25°. To build up a UV auroral image with a 30° by 120° field-of-view required 120 spacecraft revolutions, or about 12 min. In some modes of operation, a shorter image repetition time as low as 3 min was possible. The highly elliptical polar orbit of DE 1 (perigee ~ 450 km, apogee altitude ~ 4 Re) allowed views of the complete auroral oval from a number of perspectives. Useful images were made between an altitude of 1 Re and 4 Re. Examples of the auroral images obtained with SAI can be found in Frank et al. [1982].

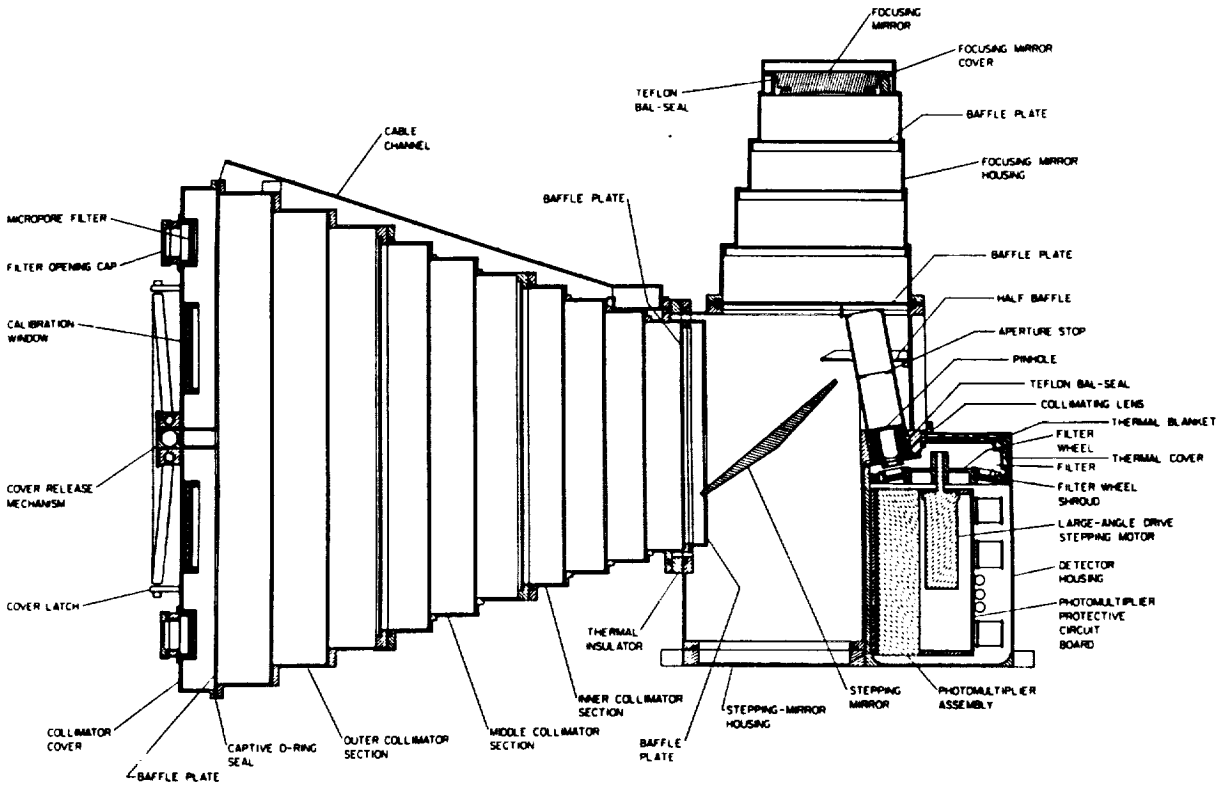

Figure 1. Detailed mechanical drawing of the cross section of one of the SAI imaging photometers which flew on DE 1.

The USAF Space Test Program/Defense Nuclear Agency HILAT (P83–1) satellite carried an instrument called the Auroral Ionospheric Mapper (AIM) [Meng and Huffman, 1984]. HILAT, a three-axis stabilized spacecraft, was placed in an 830-km circular orbit with an inclination of 82°. AIM was mounted on the bottom of the spacecraft so that it had a clear view of the Earth (fig. 2). The instrument consisted of a parabolic telescope coupled to a 1-m Ebert-Fastie spectrometer. The viewing direction of the telescope was controlled by a scanning mirror which swung 67° from one side of the nadir direction

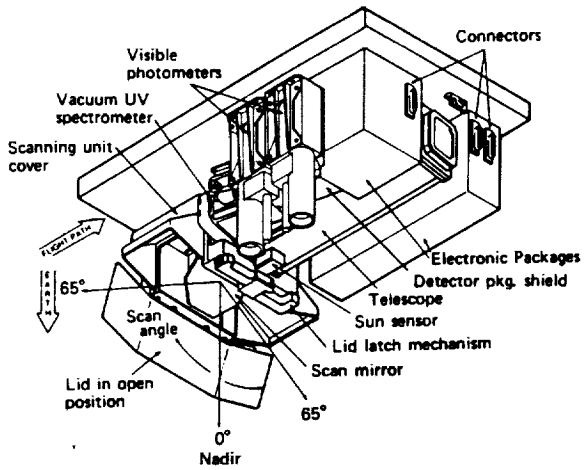

Figure 2. Schematic diagram of the auroral imager experiment for the three-axis stabilized polar orbiting HILAT satellite.

to the other. The plane through which the telescope field-of-view scanned was perpendicular to the direction of spacecraft motion so that a full image could only be built up from data gathered along a portion of the spacecraft orbit. A full scan of the mirror took 3 s, producing a ground swath 5,000 km long and about 25 km wide. The spectrometer was designed to operate in the 1,100 to 1,900 Å range with a spectral resolution of 30 Å. The detector was a solar blind EMR 510G photomultiplier tube with a CsI cathode and an MgF window. This instrument was able to image auroral features in sunlight.

An instrument similar to AIM called the Auroral Ionospheric Remote Sensor (AIRS) was launched on the *Polar Bear* spacecraft in the fall of 1986, into a near circular polar orbit at 1,000 km [Schenkel et al., 1986]. The method for creating a two-dimensional image, by scanning perpendicular to the direction of flight with a moving mirror and appending successive image strips along the line of flight, was the same as that used on AIM. The instrument had four simultaneous data collection channels, two operating in the vacuum ultraviolet and two operating in the near ultraviolet and visible. For the two VUV channels, part of the light entering the telescope was sent to an Ebert-Fastie spectrometer which had two moveable 30 Å wide slits separated by 240 Å. Light passing through these slits was detected by two separate photomultiplier tubes. The rest of the light entering the instrument is split into two beams where it is sent to one of two pairs of narrow bandpass detectors. One pair consists of two 10 Å wide bands at 3,914 and 6,300 Å. The second pair consists of a 10 Å wide band at 3,371 Å and a 200 Å wide band at 2,250 Å. Spatial resolution for the two VUV spectrometer channels was 6.5 by 26.7 km, and for the two near UV and visible channels, it was 26 by 39.3 km. The total system operates at a maximum power of 9.3 W, has a data rate of 0.844 kbps per channel, and has a total weight of 23 lb.

The V5 ultraviolet auroral imager was launched into an elliptical polar orbit on the Swedish Viking satellite in February 1986 [Anger et al., 1987a]. The V5 instrument consisted of two cameras, each with a focal length of 22.4 mm (F/1) and with fields of view of 20° by 25° (fig. 3). Each camera had an angular resolution of 0.076° by 0.076°. One of the cameras was responsive to the spectral range of 1,340 to 1,800 Å through the use of a BaF_2 filter and a CsI photocathode. The other camera operated in the 1,235 to 1,600 Å band by using a CaF_2 filter, a KBr photocathode, and reflective coatings on the secondary mirror. The large field-of-view of the cameras was obtained by use of spherical mirror surfaces. The microchannel plate detector was also curved to lay on the same spherical surface as the secondary mirror. Photons striking the photocathode, covering the surface of the microchannel plate, produced photoelectrons which were amplified by the microchannel plate. These electron pulses fell on a curved phosphor plate which then emitted light pulses which were conducted to a CCD (288 X 385) via a fiber optic conduit with a distortion corrector that mapped the curved photocathode image surface to the flat CCD image surface (fig. 4). Each camera was mounted to view out the side of the spinning spacecraft. Motion compensation was accomplished by reading out the CCD rows in step with the rotation. To do this required that the CCD columns be aligned with the spacecraft equatorial plane within 0.2°. Because this instrument did not need to scan the scene in order to build up an image, it could produce one auroral image every 20 s. There is, however, evidence to suggest that the large field-of-view resulted in scattered light problems. Images from this instrument can be seen in Anger et al. [1987b].

An ultraviolet auroral imager (UVI) has been designed and built for the ISTP Polar spacecraft [Torr et al., 1992] and is currently undergoing integration with the spacecraft (fig. 5). It consists of a single F/3, three mirror camera [Johnson, 1988]. This camera has an instantaneous field-of-view of 8° and an angular resolution of 0.03°. Because of its field-of-view, this instrument will only be able to image the whole auroral oval when it is above an altitude of 5 Re. It is designed to operate as a staring and not a scanning instrument and will be mounted on Polar's despun platform. A filter wheel, with seven filters, sits just inside the entrance of the telescope portion of the instrument. In front of this entrance is a mirror wheel with three mirrors set at a 45° angle to the entrance. These mirrors have

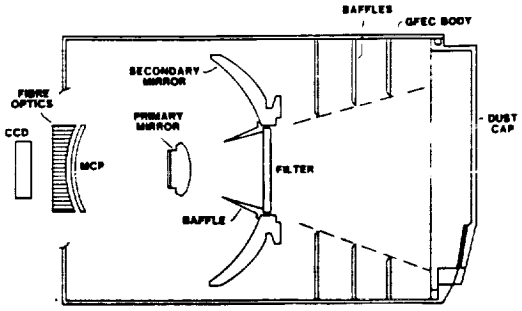

Figure 3. A schematic cross section of one of the Viking V5 cameras detailing the GFEC housing, inverse Cassegrain optics, baffles, dust cover, filter, curved intensifier, fiber optic tapers, and the CCD.

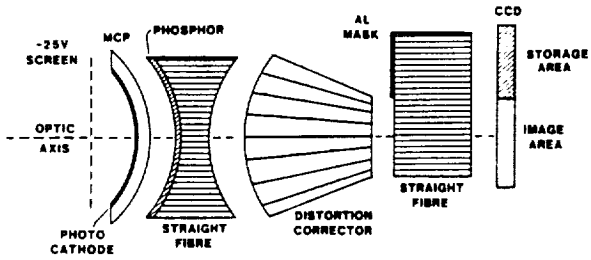

Figure 4. A schematic cross section of a V5 intensifier assembly showing the electron screen, the curved mcp and photocathode, the phosphor screen, sections of the fiber optic distortion corrector, and the CCD.

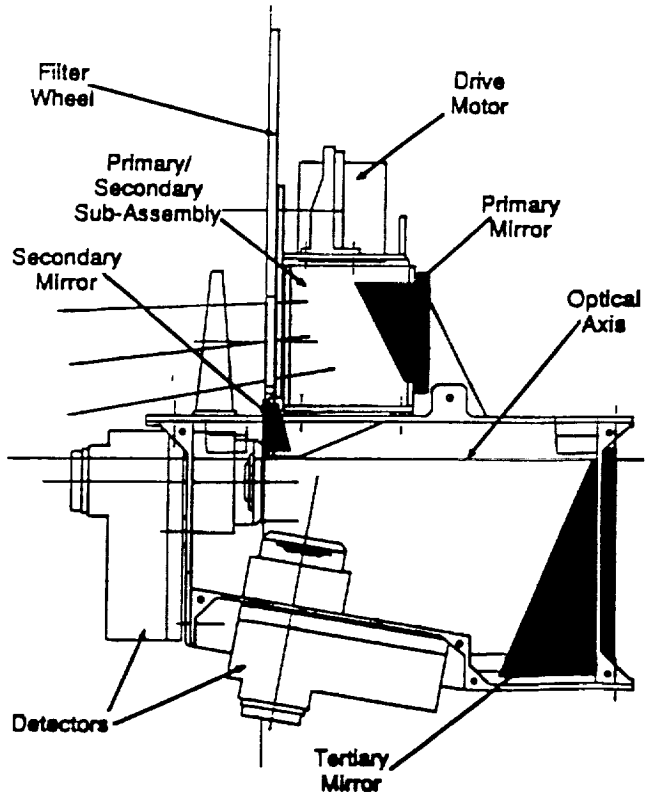

Figure 5. Schematic of the UVI instrument.

multilayer film coatings which provide some of the overall filtering through selective reflection of certain wavelengths. There are four reflection/transmission filter combinations with narrow passbands centered at: (1) the Lyman-α line at 1,216 Å, (2) 1,743 Å, (3) an atomic oxygen line at 1,304 Å, and (4) another atomic oxygen line at 1,356 Å. Two reflection/transmission filter combinations have a relatively broader passband with one designed for the short wavelength portion of the LBH band (1,450 to 1,600 Å) and the other for the long wavelength portion (1,620 to 1,850 Å). The coated mirrors of the imaging telescope are also a part of the filter system, providing superb long wavelength rejection. The detector consists of a solar-blind CsI photocathode coated microchannel plate coupled to a 244 by 206 element

CCD array. This combination of filters and detector gives a net 10^{-9} rejection of all out-of-band emissions. The three telescope mirror surfaces are coated with MgF_2 after having been ground to a very smooth finish with a surface roughness of less than 20 Å. The smooth mirrors, coupled with internal baffles, greatly suppresses stray light allowing the instrument to simultaneously image both very bright and very dim emissions. Image repetition times will vary according to the operating mode but could be as short as 30 s. A complete cycle of background measurements along with integration at each filter setting could take as long as 8 min. This instrument has a mass of 21 kg, an average power consumption of 20 W, and a data rate of 12 kbps.

The above list of auroral imagers by no means represents the state of the art. These specialized instruments continue to be improved. An SAI derivative that was proposed for MARIE in 1988 would scan the image 12 lines at a time giving a factor of 12 reduction in the length of time needed to create an image (1 min compared to SAI's 12 min). An ultraviolet auroral imager called the UVAI, which is a follow on to the Viking V5 instrument, is being developed for the Interball project. In many respects, UVAI will be very similar to V5, but a number of improvements in the filters and fiber optic correctors have been included [Adema, 1990]. The group that developed the UVI instrument for Polar continues to push ahead, redefining the state of the art. The field-of-view of the instrument can be increased to 10° or 12° with only a slight loss in angular resolution. With new optical designs, the imaging head can be made significantly smaller and lighter. It may be possible to put three imaging heads in the same volume where the single UVI head now sits. Such an arrangement would give a significant increase in field-of-view with no sacrifice in angular resolution. Most of the mass in the UVI electronics box consists of memory chips. The new RAM chips being offered by Honeywell promise a factor of 2 reduction in weight of the electronics box. It appears that the UVI or its derivatives would easily be able to meet all of the requirements for IMI.

GEOCORONAL IMAGERS

One of the strongest emission lines in the solar UV spectrum is the hydrogen Lyman-α line at 1,216 Å. Because of the abundance of atomic hydrogen near the Earth, much of this light will be scattered, creating a bright UV image. Next to the aurora, the geocorona is the easiest to image. At least two instruments have been flown which have imaged the geocorona, and they will be discussed in more detail in the following. Many rocket- and satellite-borne UV photometers and spectrometers have observed this emission but not imaged it [Meier and Mange, 1970; Young et al., 1971a]. The French D2A Tournesol satellite, launched in 1971, carried a photometer which measured Lyman α in the 456- to 712-km altitude range [Blamont et al., 1975]. Results from this experiment were used to study the hydrogen geocorona at the exobase.

In 1972, *Apollo 16* astronauts took an ultraviolet camera to the Moon which was used, among other things, to obtain UV photographs of the Earth and near-Earth space. These photographs showed atmospheric dayglow, aurora, nightside low latitude airglow bands, and the geocorona [Carruthers and Page, 1972]. The camera which took these pictures was an electronographic Schmidt f/1 system with a 75-mm aperture (fig. 6). Light entered the front of the instrument through a transmission filter/corrector plate and was focused on a photocathode (near the front of the camera) by a single reflection from the spherical primary mirror (at the back of the camera). Electrons freed from the photocathode were then accelerated to the back of the camera by a 25 kV potential and focused by a magnet surrounding the camera. This electron image was recorded on film which was later returned to Earth. The camera's filter system consisted of a KBr photocathode, which effectively eliminates light with wavelengths greater than 1,600 Å, and two corrector plates. One of the plates was made of lithium fluoride and had a short

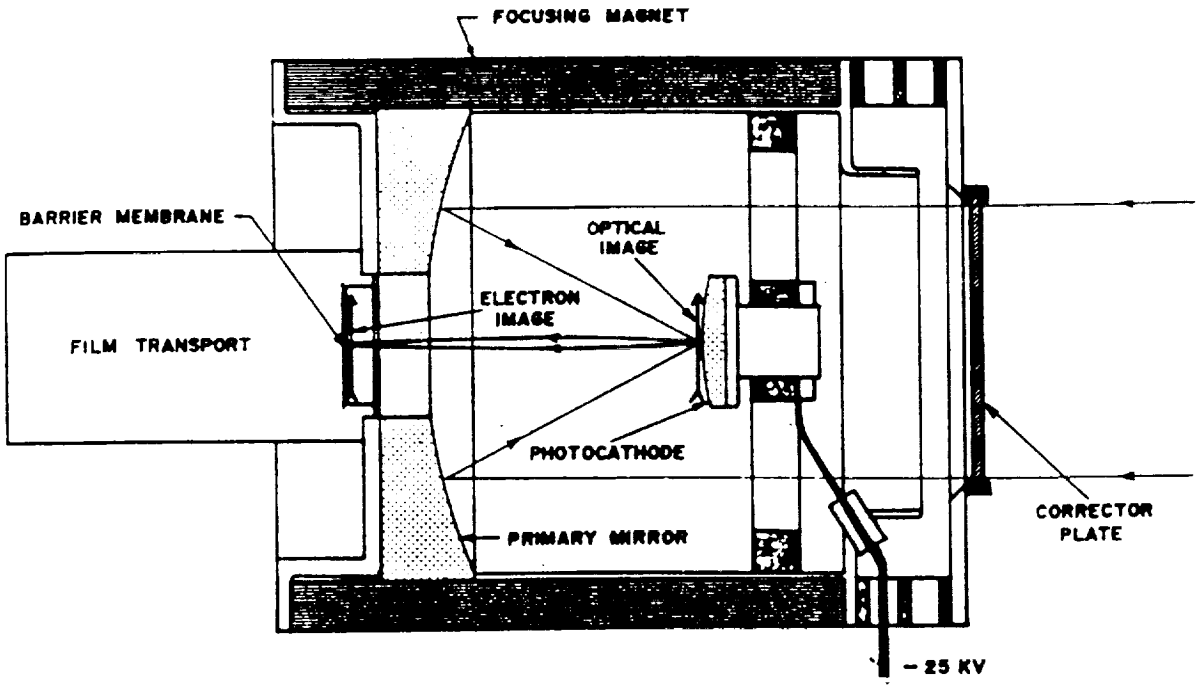

Figure 6. Simplified cross-section diagram of the electronographic Schmidt camera used by *Apollo 16* astronauts to take photographs of the geocorona from the Moon's surface in 1972.

wavelength cutoff at 1,050 Å, the other was made of calcium fluoride with a cutoff at 1,250 Å. Thus, the instrument operated in the 1,050 to 1,600 Å and 1,250 to 1,600 Å bands. Because of the spherical optics, the camera had a field-of-view of 20°, although there were some distortion problems. In addition to the imager, the instrument also included a spectrograph for isolating, but not imaging, individual spectral features [Carruthers, 1973].

The Scanning Auroral Imager on DE 1 also had the capability to image the geocorona. One of the three camera assemblies had, among its 12 filters, four which had passbands that included the 1,216 Å feature. This instrument is described above and in more detail in Frank et al. [1981]. This instrument produced many images of the geocorona between 1981 and 1985 which have been used for quantitative studies of the near-Earth hydrogen atmosphere [Rairden et al., 1986]. At the very least, an instrument like the DE 1 imager, but simplified so as to look at only the 1,216 Å feature, would be able to meet many of the requirements for the IMI geocoronal imager. Improvements would be needed in the overall instrument throughput (in order to see the geocorona to greater geocentric distances) and the use of a narrower band filter (to more effectively eliminate unwanted spectral features). Malherbe [1974] describes the performance of a narrow-band hydrogen Lyman-α filter with a peak transmittance of 15 percent and a bandwidth of 90 Å (FWHM). If one could design a 1,216 Å filter similar to the 1,356 Å filter that has been fabricated for UVI, it would have a peak transmittance of about 40 percent with a bandwidth of about 50 Å (FWHM) [Zukic and Torr, 1991]. These two filters are to be compared to the best 1,216 Å filter on SAI which had a transmittance of 14 percent and a bandwidth of about 110 Å. Recently, an imaging microchannel plate detector, optimized for 1,216 Å hydrogen Lyman α by using a KBr photocathode, was flown on a rocket experiment [Bush et al., 1991]. With the improvements in technology that have occurred since SAI was developed, it seems very possible that the IMI requirements for a geocoronal imager can be met.

He^+ 304 Å IMAGER

Although it has long been realized that measurements of the 304 Å emissions for He^+ could be used as a means of mapping the distribution of plasma in the plasmasphere [Young et al., 1971b], to date no instrument has been flown to do this type of imaging in the sense that is being proposed for IMI. A number of rocket and satellite flown instruments have detected this radiation and produced crude maps of its distribution [Meier and Weller, 1972; Weller and Meier, 1974; Parsece et al., 1974; Chakrabarti, 1982]. These measurements have established the flux levels of the 304 Å emissions and demonstrated that they do bear a relationship to the structure of the plasmasphere.

Since no past examples of a He^+ 304 Å imager exist, the only way to discuss the heritage of this instrument is in terms of the enabling technology that such an instrument would use. The basic requirements for this instrument, as identified by the science working group, are (1) high throughput at 304 Å, (2) narrow passband of 50 to 100 Å width with good out-of-band rejection, and (3) large field-of-view with an angular resolution of 0.5°. The high sensitivity at 304 Å is needed in order to see the full plasmasphere, the refilling plasmasphere, and the plasma trough. The good out-of-band rejection is needed to eliminate competing signals at 584 Å from atomic helium, 834 Å from O^+, and 1,216 Å from atomic hydrogen. The signal from atomic hydrogen is particularly strong, posing a significant challenge. The large field-of-view is needed in order to see all of the plasmasphere from a position just inside it, or just outside it.

A soft x-ray telescope, designed to fly on a polar orbiting astronomical satellite (was scheduled for a Pegasus launch in mid-1991), has many of the characteristics needed for the 304 Å camera [Bloch et al., 1990; Smith, 1990]. The experiment to be flown on this satellite is called array of low-energy x-ray imaging sensors (ALEXIS). It consists of six telescopes designed to survey the entire sky in three narrow wavelength bands at 133 Å, 171 Å, and 186 Å. Each telescope has a 33° field-of-view with an angular resolution of 0.5°. The optics are very simple and compact (fig. 7). They consist of a single

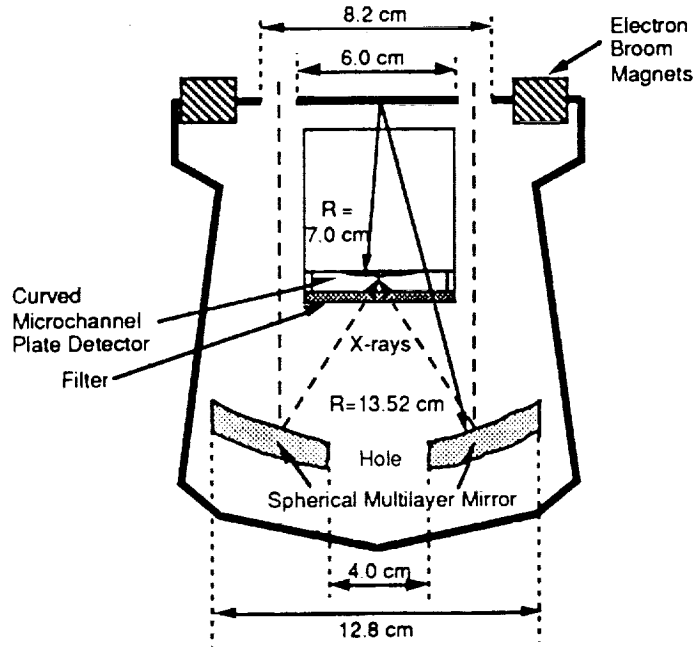

Figure 7. Cross-sectional diagram of an ALEXIS telescope.

spherical mirror which focuses light entering the telescope aperture on a curved microchannel plate detector. Before reaching the detector, the light passes through a transmission filter placed just in front of the detector. The overall filtering is accomplished through the design of the multilayer mirror, the composition and thickness of the transmission filter, and construction of the microchannel plate detector. The multilayered mirror surface consists of 40 to 60 alternating Mo-Si layer pairs. One of the challenges in coating the mirror was to assure a relatively uniform *d* spacing at all points on the highly curved surface. The researchers were able to accomplish this to within 1 percent. To eliminate the 304 Å signal from the plasmasphere (which these researchers did not want to see), they adjusted the first Mo-Si layer pair so that it formed a destructive interference cell to greatly reduce the mirror's reflectivity at 304 Å. The transmission filters for the 186 Å telescope and the 171 Å telescope consisted of a thin metallic film with 1,200 Å of aluminum and 600 Å of carbon. The filter for the 133 Å telescope used 1,500 Å of Lexan, 200 Å of titanium, and 900 Å of boron.

To make a He^+ 304 Å camera based on the ALEXIS design would require a larger field-of-view and a filtering system designed for 304 Å and not against it. According to R. Meier, the Cassegrain optical system used for ALEXIS can be designed with a larger field-of-view (40° to 45°) and have either a circular or rectangular aperture. Three such cameras would give a field-of-view of 120° to 135°. With all three cameras aligned to have their look directions pointing at angles separated by 40° to 45°, but all in the plane containing the spacecraft spin axis, the instantaneous field-of-view could be 45° by 135° with angular resolution throughout of 0.5° by 0.5°. As the spacecraft spins, this fan-shaped region would sweep through 360° giving a total field-of-view of 135° by 360°. Thus, it seems likely that the total field-of-view requirement for the 304 Å instrument could be met. To meet the filtering requirements would necessitate a different combination of multilayer mirror and transmission filter than used on ALEXIS. Among the various telescopes carried on the rocket-borne multispectral solar telescope array (MSSTA) was a Ritchey-Chrétien design optimized for viewing the solar disk at 304 Å [Barbee et al., 1991; Lindblom et al., 1991]. The mirror coatings in this telescope consisted of 26 layer pairs with 74 Å of Mo and 99 Å of Mg_2-Si. Their reflectivity at 304 Å was 25 percent with a bandwidth (full width half max) of 26 Å. The transmission filter consisted of 2,850 Å of aluminum, 60 Å of aluminum oxide, and 152 Å of carbon. It had a transmission of about 13 percent at 304 Å which dropped gradually to 0.1 percent at 900 Å. Above 900 Å, the transmission drops rapidly to 10^{-10} percent at 1,000 Å. The possibility of using other transmission filter material combinations such as tellurium and silicon or a combination of aluminum or silicon with boron or carbon has been recently investigated [Schulze et al., 1991]. One possible detector that could be used would be a curved microchannel plate with "solar blind" CsI cathode and a wedge and strip position detector anode. The design of the detector could also be optimized for detection of 304 Å and rejection of other wavelengths. Because of the flexibility in the design of multilayer mirrors, transmission filters, and detectors, it appears that there will be little difficulty meeting the IMI requirements for the He^+ 304 Å camera. Much of the technology needed for this instrument is currently being developed and advanced by the solar and astrophysics communities.

A He^+ 304 Å imager called WIDGET, based on the ALEXIS telescope design, was scheduled for a fall 1992 sounding rocket flight [Cotton et al., 1992] to test its capabilities. Although WIDGET uses the same basic optical design as ALEXIS, it will use a flat, rather than a curved, microchannel plate detector. This choice was made because of the lower cost and easy availability of the flat plates and results in a reduction of the imaging capabilities of the telescope. According to these authors, WIDGET can easily be configured to operate at other wavelengths (584 Å, 834 Å, and 1,216 Å), as well as at 304 Å by the appropriate choice of mirror coatings and filters.

O^+ 834 Å IMAGER

The possibility of imaging the Earth's magnetosphere, or portions of it, with an instrument designed to measure O^+ resonantly scattered 834 Å radiation is difficult to access. While there are many measurements of 834 Å originating in the ionosphere there are few measurements of 834 Å emissions coming from the magnetosphere [Kumar et al., 1983]. There is no doubt that such emissions may originate in the magnetosphere, but they may be too weak to see. An added problem is the fact that the sunlit ionosphere is a major source of 834 Å radiation and poses a serious contamination problem for any look direction pointed at or near the Earth. As with the 304 Å camera, no previous instrument has been flown to image O^+ in the magnetosphere. The design requirements for this instrument are identical to those for the He^+ 304 Å camera with the exception of the wavelength of peak sensitivity.

Recently Zukic et al. [1991] (also Zukic et al., 1992) proposed a design for an 834 Å magnetospheric imaging camera based on their work developing the UVI optical system and filters. The heart of the design is a method for creating a narrow passband filter centered at 834 Å. This is accomplished mainly by the multilayer coatings on the three mirrors in the instrument. Each coating is designed so as to be highly reflective at 834 Å over the range of angles at which light strikes that mirror. The transmittance of the three-mirror system at 834 Å is 20 percent, with a bandwidth of 68 Å (fig. 8). At 304 Å, the transmittance is 0.03 percent, at 584 Å it is 0.05 percent, and at 1,216 Å it is 0.004 percent. These results are achieved by the combined effect of the filtering that occurs at each mirror reflection. The use of a bare microchannel plate detector greatly aids in the reduction of Lyman α making a large signal-to-noise ratio possible. Theoretically, the instrument could achieve a signal-to-noise ratio of 10 for a 0.01 R signal in 8.8 s for the full 6° field-of-view. The 6° circular field-of-view, however, is far below what is required for IMI. It may be possible to get a larger field-of-view in one direction by using a series of these cameras. To get the 135° needed would require 23 of these cameras in series. If, however, their individual fields-of-view could be increased to 12° (as appears possible for a Polar UVI derivative), then only 11 or 12 would be needed. If they could be made smaller than the UVI camera, along the lines currently envisioned by Torr's group, then 12 such cameras would have the mass

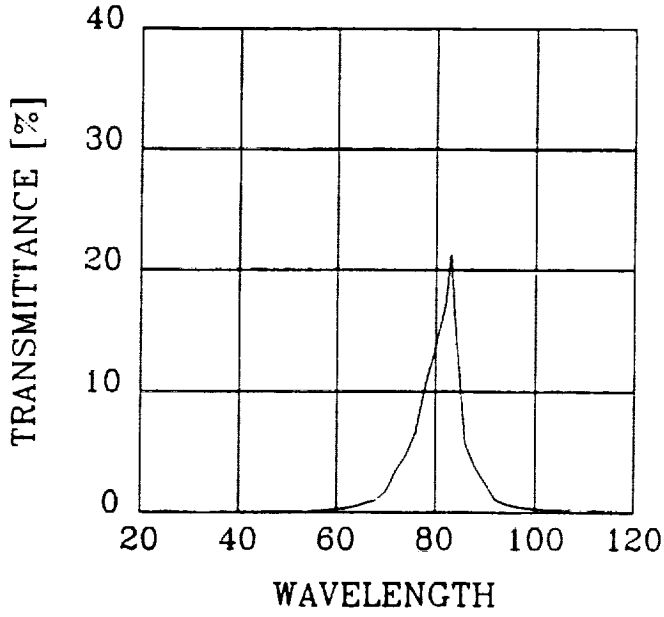

Figure 8. The calculated transmittance of the 83.4-nm self-filtering camera [Zukic et al., 1991].

and volume of four UVI cameras. Because of its heritage in UVI, this proposed 834 Å camera would, however, be ideally suited to be a staring instrument mounted on the despun platform, should it be decided that is what is needed.

R. Meier envisions an 834 Å camera similar to the 304 Å camera based on the ALEXIS Cassegrain telescope. Such may be possible with the right multilayer mirror coating, transmission filter, and detector. A multilayer mirror based on the design of Zukic (discussed above) might be used for this camera as well. Such a mirror would have a reflectivity of 60 percent at 834 Å and about 8 percent at 1,216 Å. Since the ALEXIS design uses only one mirror, the rejection of 1,216 Å light is not as good with this design as it is with the Zukic design. No doubt, if an ALEXIS design is to be used, the design of the multilayer mirror will need to be revisited. Recent work by Chakrabarti et al. [1992] represents some initial efforts in this direction. The ALEXIS telescope also uses a transmission filter to block long wavelengths. Transmission filters have been designed for wavelengths throughout the vacuum ultraviolet and extreme ultraviolet region, and it does not seem unreasonable to expect that they could be designed for 834 Å as well, although the author is not aware of any work that has been done on this. Whatever the final design, the instrument would need the highest possible throughput since the signal may be very weak. It would also need a large dynamic range in order to see weak emissions from the plasmasphere alongside the strong emissions from the ionosphere [Gladstone, 1992].

ELECTRON PRECIPITATION IMAGER

The first satellite observations of bremsstrahlung radiation (x rays) produced by precipitating auroral electrons were made from an instrument flown on the 1972–076B satellite [Imhof et al., 1972]. The satellite, launched on October 2, 1972, was placed into a nearly circular Sun-synchronous orbit at an altitude of 750 km and an inclination of 98.4°. The detector was a Ge(Li) spectrometer sensitive to photons with energies between 50 keV and 2.6 MeV. It had a ±20° acceptance cone pointed nearly radial to the spacecraft spin axis, allowing the spectrometer to view the ground once every spacecraft rotation. The only imaging done by this instrument was done by compiling the instrument output from along its orbital path.

The x-ray spectrometer instrument carried on the second DMSP (F2) satellite of the block 5D series (1977–044A) used a proportional counter and an array of four cadmium-telluride detectors as the sensing elements [Mizera et al., 1978]. The proportional counter was sensitive to x rays from 1.4 to 20 keV, while the cadmium-telluride sensors covered the energy range from 15 to 90 keV. The proportional counter was a nadir viewing instrument with a field-of-view of ±2° along the satellite track and ±14° cross track. Spatial imaging is done in the same way as on the 1972–076B satellite. Fifteen energy channels between 1.4 and 20 keV are used for x-ray spectral information. The four cadmium-telluride semiconductor detectors had five energy channels and were placed so as to give some direction finding capability.

The DMSP–F6 satellite, in a Sun-synchronous 830-km orbit (launched December 20, 1982), carried a scanning x-ray spectrometer which produced the first true images of x-ray aurora [Mizera et al., 1984]. This instrument measured differential fluxes in the energy range between 2.0 and 78 keV in 23 channels. The sensor element was a single wire, 3 atmosphere proportional counter containing equal amounts of argon and xenon gases. It was mounted on a scanning head that swept a 5° by 10° (FWHM)

collimator from limb to limb in 10 s. This cross-track scanning, combined with the 7-km/s spacecraft motion produced a raster image with a pixel size of approximately 70 by 130 km at an altitude of 100 km.

The X-ray Imaging Spectrometer (XRIS) instrument obtained worldwide x-ray images from the S81–1 spacecraft from May 26 to July 2, 1982 [Imhof et al., 1985]. This instrument used a position-sensitive proportional counter and a pinhole camera to form a one-dimensional 16-pixel image [Calvert et al., 1985]. It was mounted so that it looked forward and downward from the three-axis stabilized S81–1 spacecraft. Because of the satellite's low-altitude orbit (170 to 280 km) and the instrument's 7° by 90° field-of-view, it produced images with spatial resolution of 30 km by about 1 km. The counter was filled with xenon gas and was sensitive to x rays between 4 and 40 keV. The center two image pixels returned energy spectra over 24 channels, while the remaining pixels used eight channels.

The ISTP Polar spacecraft will carry an x-ray imaging spectrometer instrument called Polar ionosphere x-ray imaging experiment (PIXIE) [Imhof et al., 1991; Imhof et al., 1992; McKenzie et al., 1992]. This instrument will be mounted on the despun platform and will image the x-ray aurora from altitudes of 1 to 8 Re (fig. 9). The optical system is a multiple pinhole camera with movable plates which can change the pinholes used during different portions of the orbit as the distance from the image changes. At high altitudes, the camera will have 16 open holes which will produce 16 separate auroral images on the image detector. These will be added to form a single image. As the spacecraft comes down in altitude, fewer holes will be open, producing fewer but larger images with high angular resolution. The detector consists of a two-cell, position-dependent, proportional counter. It is 180 by 180 mm with a 2-mm spatial resolution that will give an angular resolution of about 0.5° over the

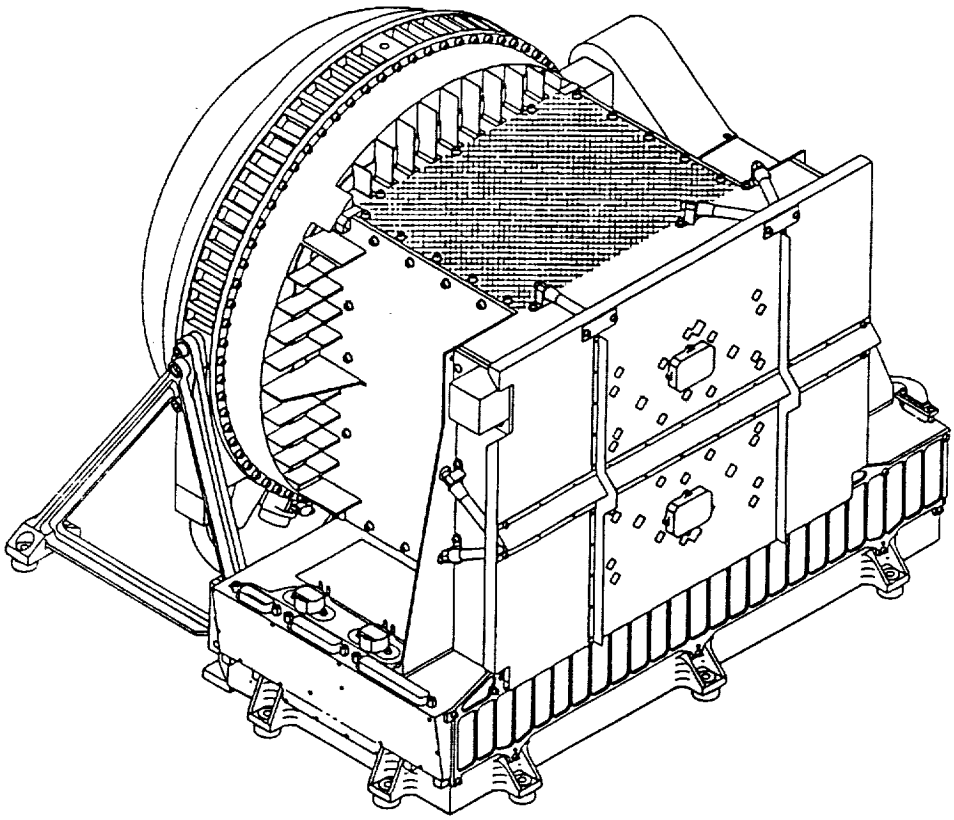

Figure 9. The PIXIE instrument.

40° field-of-view. The front cell is filled with argon at one atmosphere, and the back cell is filled with xenon at two atmospheres. Both cells use CO_2 as a quencher gas. With these choices of gases and the thicknesses of the entrance windows, this detector is sensitive to photons in the 3 to 60 keV energy range. In operation, this instrument will telemeter to the ground 24 bits of position and energy information for every x-ray event. In this way, various types of composite images and time exposures could be made while the data are analyzed.

The PIXIE instrument is the closest heritage available for the IMI electron precipitation imager. It is, however, an untested instrument, and several people have expressed their doubts about how well it will work [G. Parks, private communication]. Even if it works as planned it will still fall short of the IMI requirements in that its energy range will be too high (3 to 60 keV compared to 0.3 to 10 keV) and, because of the positional sensitivity of its proportional detector (2 mm), will likely have an angular resolution that is too large (~0.5° compared to 0.02°). The performance of PIXIE might be improved through the use of upgraded proportional counters such as those being developed for the Japanese ASTRO-D mission which can detect x rays down to 0.7 keV with a 0.5-mm positional resolution [Ohashi et al., 1991]. The use of ultrathin soft x-ray windows [Viitanen et al., 1991] could further reduce the lowest energy detectable to 0.2 to 0.3 keV. In place of a proportional counter, one could use a microchannel plate detector. Bare mcp detectors have low detection efficiencies in the soft x-ray region (0.1 to 10 keV) with no energy discrimination. However, microchannel plates with CsI photocathodes have shown efficiencies near 50 percent in this spectral range and can be operated so as to give energy spectral information [Fraser and Pearson, 1984]. The energy resolution is not as good, however, as a proportional counter. The next generation of x-ray telescopes (JET-X, AXAF, XMM) plans to use CCD's which will give improved performance compared to microchannel plates and gas proportional counters [Bräuninger et al., 1991; Wells et al., 1991].

All of the auroral x-ray imaging instruments to date use pinhole camera optics. In addition to detector improvements, overall instrument performance might be improved by the use of an optical system which uses a normal incidence, multilayer mirror telescope. Such an instrument, if it could be built, would have much higher throughput, for viewing fainter x-ray fluxes, and much better angular resolution. Multilayer mirrors for the 1 to 40 Å wavelength band (0.3 to 10 keV) are difficult to produce, but progress is being made [Kearney et al., 1991]. Most x-ray telescopes that operate in this wavelength region use grazing incidence mirrors. For example, a soft x-ray telescope designed to operate in the 4 to 50 Å range is now taking pictures of the Sun from a Japanese solar x-ray satellite (YOHKOH) [Bruner et al., 1989]. It could, in principle, perform the task of imaging electron precipitation, but it has two rather serious drawbacks. The instrument is large (1.7 m in length) because of the long focal length (1.55 m) and the inability to fold the optics of a grazing incidence telescope. It also has a small field-of-view, again because of the type of mirror used.

PROTON AURORA IMAGER

The basic idea behind the proton auroral imager has been around for a number of years. It is that energetic protons flowing into the atmosphere will charge exchange with atomic hydrogen to produce energetic, generally downflowing, hydrogen atoms. These atoms, some of which will be in excited states, will radiate photons which will be Doppler shifted when viewed by an observer who is stationary with respect to the Earth. These emission features will also be broadened because of the energy and pitch angle distributions of the precipitating protons. Observation of these Doppler shifted and broadened emission lines can give information about the proton precipitation flux as well as the energy distribution of these particles. Ground-based observations of hydrogen Balmer series emissions (Hβ–4,861 Å) have

been studied for a number of years and have established the basic features of proton aurora as well as the viability of studying them via their hydrogen emissions [Zwick and Shepherd, 1963; Eather, 1967]. These observations generally show that Hβ emissions are blue shifted (an observer on the ground sees the energetic hydrogen atoms coming toward him) by about 6 Å and broadened to about 15 to 20 Å.

The first satellite observations of Doppler-shifted hydrogen Lyman α were made in 1978 by the AFGL UV background experiment spectrometer flown on the S3–4 satellite [Ishimoto et al., 1989] in a highly inclined (i = 96.5°) low altitude (160 to 260 km) orbit. These observations show auroral Lyman-α profiles that are red shifted by about 2 to 4 Å and broadened by about 2 Å compared to the geocoronal Lyman-α emissions as seen by this instrument. To obtain the emission profiles of the proton aurora, these experimenters had to subtract an estimated geocoronal profile from their observed spectral profiles. The relatively low spectral resolution of the data used in their study made it difficult to separate the Lyman-α contributions from the proton auroral and the geocorona. The spectrometer used by Ishimoto et al. is described in two reports by Huffman et al. [1979; 1980]. A diagram of the instrument appears in figure 10. It consisted of two 1/4-m, f/5, Ebert-Fastie units scanning wavelength by a shared grating drive. One unit handled the VUV range (1,070 to 1,930 Å) and the other the UV range (1,620 to 2,900 Å). A full spectral scan tool 22 s. In both the VUV and UV ranges, three selectable bandwidth slits of 1, 5, and 25 Å were available. Photon detection was accomplished for each range by photomultiplier tubes. The VUV unit used an EMR 542G–08 detector with a CsI cathode and an LiF window, while the UV unit used an EMR 542F–08 detector with a CsTe cathode and an LiF window. The instrument had an 11.5° square field-of-view which was always directed toward the center of the Earth (nadir direction) to within 1°. (The S3–4 spacecraft was three-axis stabilized.) This instrument was not an imaging instrument since it had no focusing optics nor an array detector.

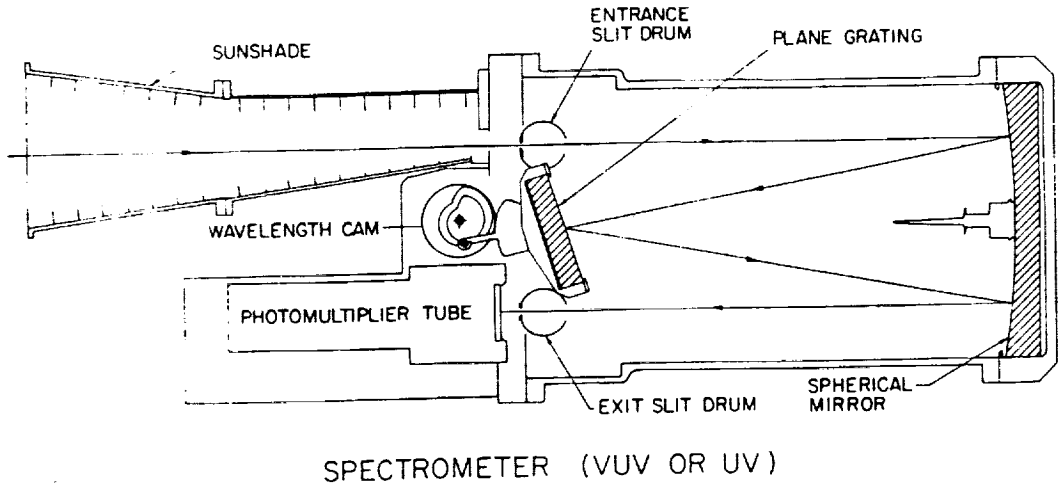

Figure 10. Drawing of the VUV background spectrometer flown on the DOD satellite S3–4 in 1978.

The observation of Doppler-shifted Lyman-α from Jupiter [Clarke et al., 1988] by the IUE satellite has motivated efforts to obtain high spatial and spectral resolution images of Jupiter in order to study proton aurora there. The Jovian auroral spectrometer rocket (JASPR) experiment was designed to measure spatially resolved far ultraviolet emission features from Jupiter at high spectral resolution (~0.04 Å) and a high sensitivity (1 to 10 Rayleighs) [Bush et al., 1991; Harris et al., 1992]. This instrument consists of a Cassegrain telescope with modified Fastie echelle spectrometer at the focal

plane. The telescope had a field-of-view of about 5 arcmin with an angular resolution of 2 to 3 arcsec. The spectrometer uses a flat (69 lines/mm) grating operating in the 224th order for 1,216 Å. The focal plane detector consists of a stack of four microchannel plates and a wedge-and-strip anode. The top plate is covered with a KBr photocathode to enhance the quantum efficiency at 1,216 Å. The first flight of JASPR occurred on May 4, 1991, but because of a star tracker malfunction the instrument was not able to acquire Jupiter. However, it did obtain useful observations of the geocorona and the interplanetary and interstellar hydrogen. The spectrometer was able to spectrally separate the geocoronal Lyman-α emissions from the interstellar emissions.

The JASPR instrument demonstrates that a high resolution spectrograph operating in the vicinity of the hydrogen Lyman-α line can be built and operated on a space platform. To produce a proton aurora imager for IMI, one could use the JASPR spectrograph, but a different front end imaging telescope would be needed. An ALEXIS telescope would have a large enough field-of-view (33°) but would not have sufficient angular resolution (0.5° compared to 0.06° called for by the IMI SWG). An imaging system like that used on the DE 1 SAI instrument would have a large field-of-view, but its angular resolution would be about a factor of 4 too large (0.25°), and it would have to operate from the spinning portion of the spacecraft. From this position, it may not be able to collect sufficient photons in a reasonable length of time to be useful. An imaging head modeled on the three-mirror UVI telescope on Polar could have an 8° to 12° field-of-view with a 0.03° to 0.05° angular resolution. An array of four miniaturized versions of these telescopes could produce an instrument with a field-of-view of about 20° by 20° with an angular resolution of about 0.05° by 0.05°. It may be difficult, however, to connect such an array to a single spectrometer.

ENERGETIC NEUTRAL ATOM (ENA) IMAGING

I. High-Energy (20 to 1,000 keV) Neutral Imaging

To date, no one has flown an instrument designed specifically for imaging energetic neutral atoms. The idea, however, has been around for about 16 years. For the terrestrial magnetosphere, the flux of energetic neutrals is produced by trapped energetic ions (mainly H^+ and O^+) which charge exchange with hydrogen atoms in the geocorona. In this reaction, the energetic ion takes an electron from a hydrogen atom but exchanges very little energy with it. The resulting high-energy neutral can then travel in a straight line (like photons) bearing information about the ion's spatial distribution, energy distribution, and composition in the region where the neutral atom was created. Energetic neutral atoms have been detected by energetic ion detectors which (although not designed for this task) were able to respond to ENA. Hovestadt and Scholer [1976] suggest that the persistent antiearthward flux of 300 to 500 keV ions seen during very quiet times by the charge particle measurements experiment (CPME) on IMP 7 [Krimigis et al., 1975] were really fluxes of energetic atoms. Since energetic neutrals could also be produced in the magnetospheres of the outer planets, the data from the low-energy charged particle experiment (LECP) on Voyager 1 were searched, and evidence was found for the detection of energetic neutrals coming from both Jupiter and Saturn [Kirsch et al., 1981a,b]. Further analysis of IMP 7 and 8 energetic particles experiment (EPE) data (>50 keV) and ISEE 1 medium energy particles instrument (MEPI) data (>24 keV) has confirmed the hypothesis of terrestrial energetic neutral atom detection [Roelof et al., 1985] and has allowed the construction of a few course ring current images [Roelof, 1987]. The ion mass spectrometer (IMS-HI) on CRESS has the capability to detect not only ions but neutrals as well and, with spacecraft spin and orbital motion, could, in principle, "raster scan" a

portion of the magnetosphere. But, due to a low duty cycle, this instrument has not produced much data for imaging purposes [Voss et al., 1992].

Because of this initial success with energetic neutral atom imaging, a great deal of interest has been generated in this field, and much work has been done designing ENA imager instruments and testing their basic components. Any instrument that would serve as an imager would need to do most, if not all, of the following tasks: (1) determine as precisely as possible the direction of travel of the neutral atom when it arrives at the spacecraft, (2) determine the energy of the neutral, and (3) determine the type (or mass) of the atom. Since these instruments would be open to space, they would need to be designed so as to reject low- to medium-energy ($\leq$1 MeV) ions and electrons, photons, and cosmic rays. These rejection tasks could be performed by the use of a variety of metal foils, electrostatic traps, and anticoincidence techniques. The components and techniques used in these instrument designs are based on tried and successful components and techniques used in charge particle detectors.

The source-loss/cone energetic particle spectrometer (SEPS) instrument, to be flown on the despun platform on the ISTP Polar spacecraft, will have the capability to image electrons, ions, and neutrals [Voss et al., 1992]. The instrument is primarily designed to image ions and electrons, but, over the polar cap, it will be able to image ENA coming from the ring current. It looks in both the nadir and zenith directions with a 24° by 28° field-of-view. The ion/neutral telescope on SEPS has 128 XY pixel elements over a 1-in^2, 200-micron deep solid state detector which is designed for the energy range of 30 keV to 10 MeV. A SiLi detector is placed behind the XY detector for use in anticoincidence rejection of penetrating radiation while a broom magnetic at the instrument aperture excludes electrons. The SEPS electron telescope can measure neutrals above 300 KeV using 256 pixels in a 2 in^2 area. It has an adjustable aperture which allows the instrument to change its spatial resolution as desired. The SEPS instrument is quite small, with a mass of 3.4 kg, a power consumption of 3.5 W, and a telemetry rate of 1.2 kbps.

The SAC-B satellite, scheduled for a mid-1994 Pegasus launch, will carry an instrument called imaging particle spectrometer for energetic neutral atoms (ISENA) [Orsini et al., 1992]. Because the satellite will be three-axis stabilized, ISENA will stare in a fixed antisunward direction. Images of the ring current will be obtained when SAC-B is on the nightside of its 500-km, low-latitude circular orbit. ISENA has two sensors, one for imaging (energetic neutral particle imager–ENPI) and the other for determining particle velocity and mass (energetic neutral particle analyzer–ENPA). ENPI consists of two modules each with identical 60° by 4° fields of view. Together they give the instrument a 60° by 8° instantaneous field-of-view. Particles entering the instrument pass through a coded aperture (which is the optical system) with six transmitting elements. This is then imaged onto a 31-element array giving each module a 2° by 4° angular resolution. The imaging sensor measures a particle's termination point using a microchannel plate followed by a position-sensitive anode. The analyzing sensor (ENPA) measures an atom's energy with a solid-state detector and uses time-of-flight to determine its mass. Ions and electrons are excluded from the instrument by a charge-deflection plate. Two thin foils at the coded aperture stop most of the UV photons. Anticoincidence in the time-of-flight sensor is used to eliminate cosmic-ray and photons which penetrate the instrument. The instrument sensor has dimensions of 22 by 29 by 6 cm, the electronics box has dimensions of 20 by 24 by 10 cm, the overall mass is 6.4 kg with a power usage of 8 W. The instrument will be sensitive to ENA between 5 and 200 keV. Figure 11 is a diagram of ISENA.

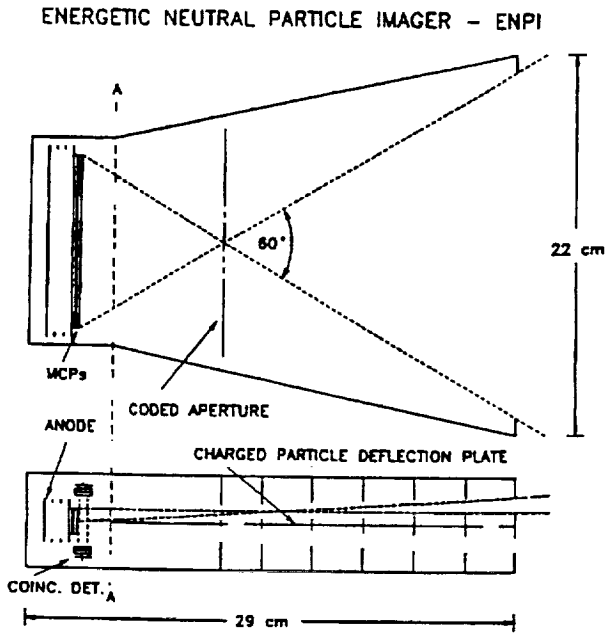

Figure 11. The ISENA ENA camera for the SAC-B satellite.

A concept instrument, also called ISENA, was proposed at the 1988 Yosemite meeting [Curtis and Hsieh, 1989; Hsieh and Curtis, 1989]. Imaging in this instrument is accomplished by use of a fan-shaped set of collimators and a coded aperture. The collimators constrain the direction of arrival in one dimension while the coded aperture constrains the orthogonal direction. The instrument would have a 45° by 45° field-of-view with, in principle, an angular resolution of 0.5° by 0.5°. After passing through the collimator, the atom passes through two thin foils (first, 83 Å Au+824 Å C; second, 275 Å C) and two time-of-flight chambers. The first chamber is 8.7 cm long while the second is 5.25 cm in length. Following the second chamber is a solid-state detector (fig. 12). Because of the different ways in which

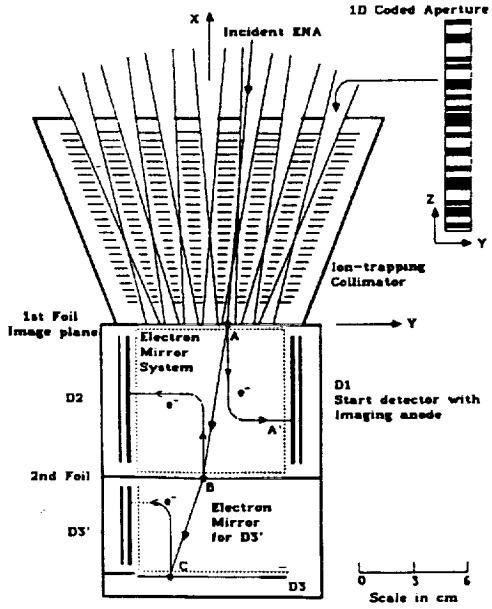

Figure 12. The ISENA concept instrument using collimator and coded aperture optics and two time-of-flight chambers for mass and energy discrimination.

hydrogen and oxygen atoms are scattered by the foils, atoms with the same velocity would have a different set of travel times across the two chambers. This information, combined with the response of the solid-state detector, will allow mass and energy discrimination. The use of two time-of-flight chambers allows very effective anticoincidence discrimination to be used to all but eliminate background from energetic ions, cosmic rays, UV photons, and random events. Low-energy ions (<160 keV) are excluded by alternating bias potentials applied to the entrance collimators. The instrument could detect H atoms with energies between 8 and 100 KeV, and O atoms between 60 and 400 keV.

A number of groups are currently working on various ENA camera concepts. Four of these include: (1) a collimated scanning telescope, (2) a pinhole camera, (3) a slit imager, and (4) a trajectory and composition analyzing instrument [McEntire and Mitchell, 1989; Keath et al., 1989]. The collimating scanning telescope (employed in the MEPI instrument on ISEE 1 [Williams et al., 1981]) collimates its field-of-view to one pixel and scans in angle to build up a complete image. Instruments (2) to (4) are illustrated in figure 13a–c. The ENA pinhole camera (fig. 13a) is designed for a staring platform. A start signal is created when the atom passes through the foil at the entrance aperture, and a stop signal is generated when it penetrates a second foil placed just above a two-dimensional microchannel plate detector. The fan-shaped set of plates acts only to exclude ions and electrons. The slit imager (fig. 13b) is a simple modification of the pinhole approach for use on a spinning spacecraft. (A version of this camera was recently proposed for a small explorer class magnetospheric imaging satellite (MARIE).) In place of a large two-dimensional field-of-view, it has a fan-shaped field-of-view. In all other respects it is similar to the pinhole camera. The trajectory and composition imager (fig. 13c) measures the direction of travel of incoming atoms by measuring where they cross a foil and impact a solid-state detector array. It thus accomplishes the basic camera function not by restricting the arrival of particles at the image surface to those which come from only one point in the sky, but by measuring the direction of arrival of the atom and then binning events on that basis. Nearly all of the high energy ENA camera designs require particles to pass through some combination of thin foils. This is what often determines the low-energy cutoff from those instruments, which often lies between 10 and 30 keV.

II. Low-Energy (0.1 to 50 keV) Neutral Atom Imaging

The ability to image neutral atoms whose energies are less than 20 keV would open up the possibility of imaging portions of the magnetosphere that an ENA camera could not see (i.e., plasma sheet, low-energy ring current, magnetosheath). There is no direct heritage for this instrument, but there are a few groups who are actively pursuing the development of at least two instrument designs. The design devised by D. McComas and colleagues at Los Alamos involves the conversion of low-energy neutrals to ions in a very thin foil and the subsequent analysis of the resulting ions with an electrostatic analyzer [McComas et al., 1992] (fig. 14). This approach may work well for atoms in the 1 to 20 keV range. It has required experimental work to characterize the interaction of low-energy atoms with thin foils [Funsten et al., 1992]. A second approach uses the way atoms interact with a surface during collision as the basis for detection [Herrero and Smith, 1992]. After striking a crystalline surface at a glancing angle, low-energy atoms are ionized and reflected in a narrow cone. These ions are then analyzed in an electrostatic analyzer which also performs the task of removing neutral particles and UV photons (fig. 15). This approach promises to be able to detect atoms with energies between 0.1 and 10 keV.

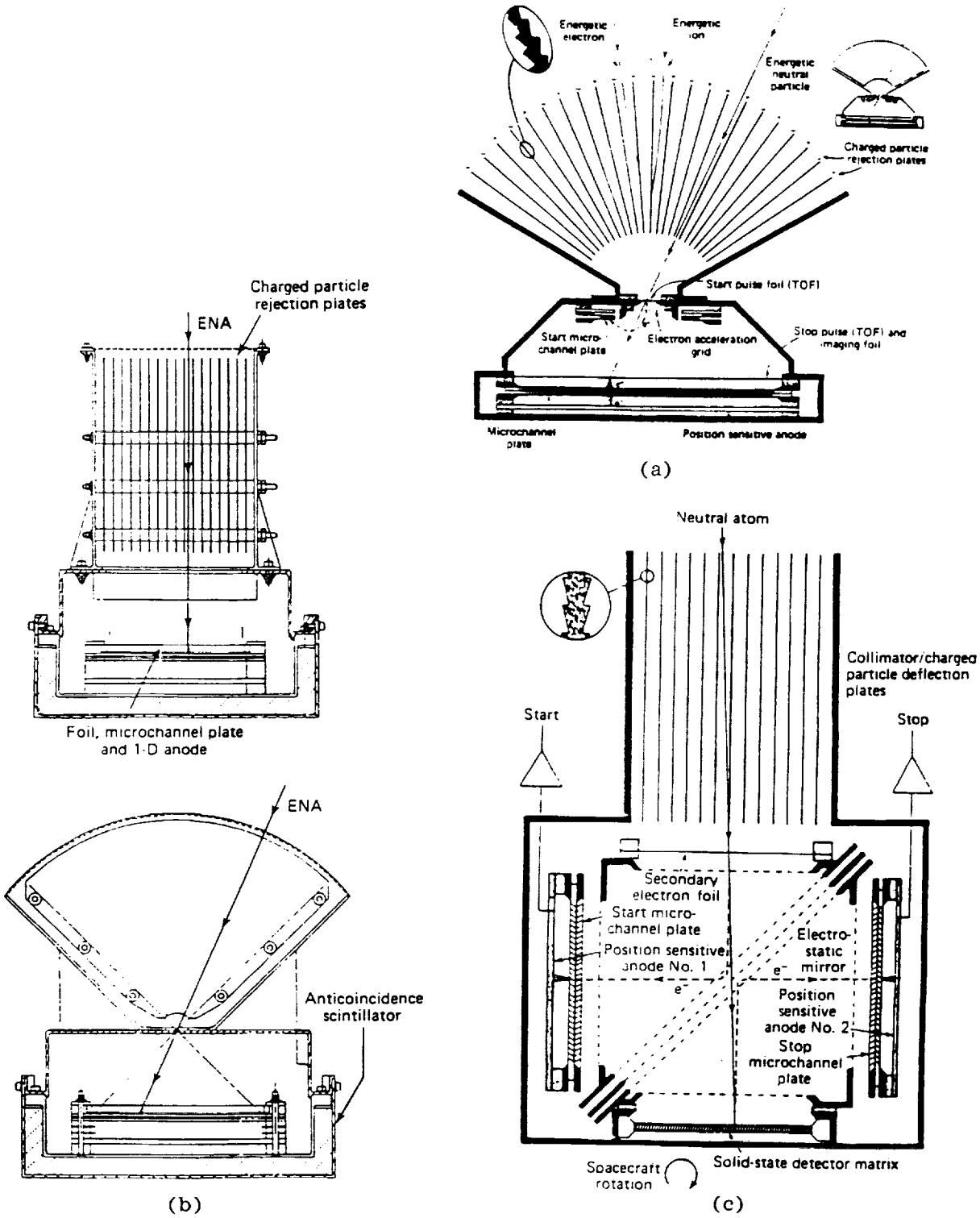

Figure 13. Several ENA camera concepts. (a) Pinhole Camera, (b) Slit Imager, (c) Trajectory and Composition Analyzing Imager.

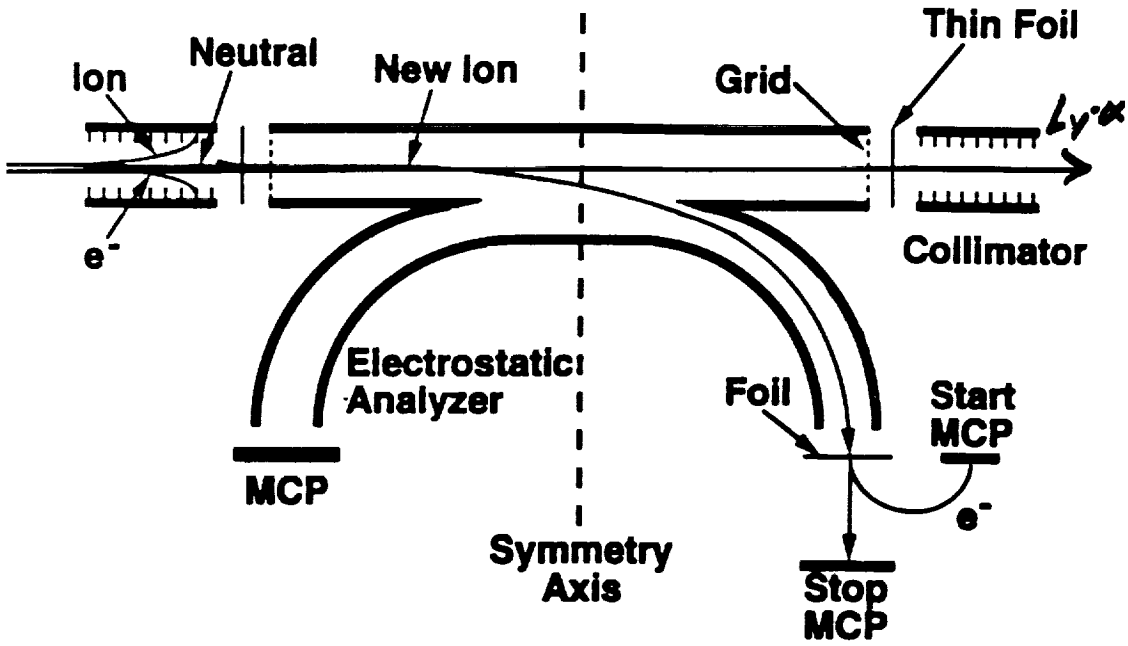

Figure 14. A diagram depicting the McComas low-energy neutral atom imager concept.

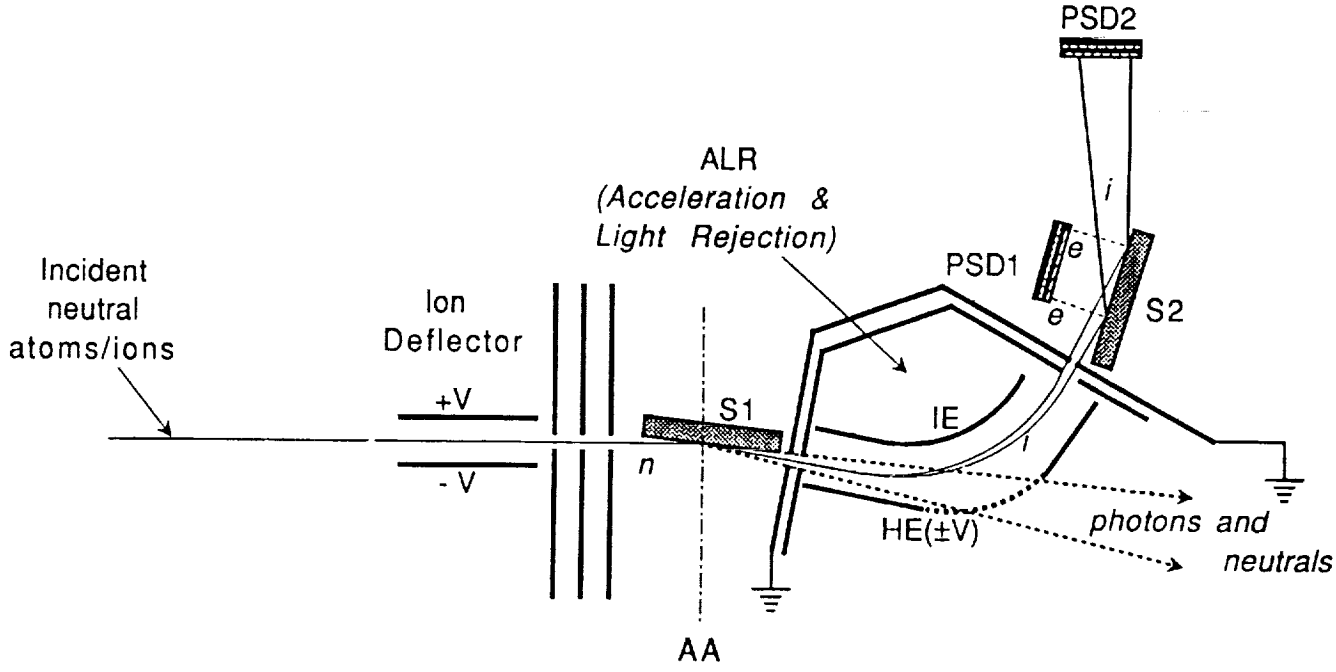

Figure 15. The Herrero LENA imager concept.

REFERENCES

Adema, J.: "Development of an Ultraviolet Auroral Imager," SPIE, vol. 1344, p. 165, 1990.

Anger, C.D., Fancott, T., McNally, J., and Kerr, H.S.: "ISIS-II Scanning Auroral Photometer," Applied Optics, vol. 12, p. 1753, 1973.

Anger, C.D., et al.: "Scientific Results From the Viking Ultraviolet Imager: An Introduction," Geophys. Res. Lett., vol. 14, p. 383, 1987a.

Anger, C.D., et al.: "An Ultraviolet Imager for the Viking Spacecraft," Geophys. Res. Lett., vol. 14, p. 387, 1987b.

Barbee, T.W., Jr., et al.: "Multispectral Solar Telescope Array II: Soft X-Ray/EUV Reflectivity of the Multilayer Mirrors," Optical Eng., vol. 30, p. 1067, 1991.

Blamont, J.E., Cazes, S., and Emerich, C.: "Direct Measurement of Hydrogen Density at Exobase Level and Exospheric Temperatures From Lyman α Line Shape and Polarization 1. Physical Background and First Results on Day Side," J. Geophys. Res., vol. 80, p. 2247, 1975.

Bloch, J.J., et al.: "Design, Performance, and Calibration of the ALEXIS Ultrasoft X-Ray Telescope," SPIE, vol. 1344, p. 154, 1990.

Bräuninger, H., et al.: "Progress With PN-CCD's for the XMM Satellite Mission," SPIE, vol. 1549, p. 330, 1991.

Bruner, M.E., Acton, L.W., Brown, W.A., Stern, R.A., Hirayama, T., Tsuneta, S., Watanabe, T., and Ogawara, Y.: "The Soft X-Ray Telescope for the Solar A Mission," in Solar System Plasma Physics, eds. Burch, Waite, and Moore, p. 247, AGU, Washington DC, 1989.

Bush, B.C., Cotton, D.M., Siegmund, O.S., Chakrabarti, S., Harris, W., and Clarke, J.: "High Resolution, Two-Dimensional Imaging, Microchannel Plate Detector for Use on a Sounding Rocket Experiment," SPIE, vol. 1549, p. 290, 1991.

Calvert, W., Voss, H.D., and Sanders, T.C.: "A Satellite Imager for Atmospheric X-Rays," IEEE Trans. Nucl. Sci., vol. NS-32, p. 112, 1985.

Carruthers, G.R., and Page, T.: "Apollo 16 Far-Ultraviolet Camera/Spectrograph: Earth Observations," Science, vol. 177, p. 788, 1972.

Carruthers, G.R.: "Apollo 16 Far-Ultraviolet Camera/Spectrograph: Instrument and Operations," Applied Optics, vol. 12, p. 2501, 1973.

Chakrabarti, S., Paresce, F., Bowyer, S., Chiu, Y.T., and Aikin, A.: "Plasmaspheric Helium Ion Distribution From Satellite Observations of He II 304 Å," Geophys. Res. Lett., vol. 9, p. 151, 1982.

Chakrabarti, S., Edelstein, J., Keski-Kuha, R.A.M., and Threat, F.T.: "An 834 Å Reflective Coating for Magnetospheric Imagery Applications," SPIE, vol. 1744, p. 208, 1992.

Chubb, T.A., and Hicks, G.T.: "Observations of the Aurora in the Far Ultraviolet From OGO 4," J. Geophys. Res., vol. 75, p. 1290, 1970.

Clarke, J.T., Trauger, J., and Waite, J.H. Jr.: "Doppler Shifted H Lyα Emission From Jupiter's Aurora," Bulletin of the American Astronomical Society, vol. 20, No. 3, p. 898, 1988.

Cotton, D., Conant, R., and Chakrabarti, S.: "The WIDe-angle GEocoronal Telescope (WIDGET)," SPIE, vol. 1744, p. 110, 1992.

Curtis, C.C., and Hsieh, K.C.: "Remote Sensing of Planetary Magnetospheres: Imaging Via Energetic Neutral Atoms," in Solar System Plasma Physics, eds. Burch, Waite, and Moore, p. 247, AGU, Washington DC, 1989.

Eather, R.H., "Auroral Proton Precipitation and Hydrogen Emissions." Rev. Geophys., vol. 5, p. 207, 1967.

Frank, L.A., Craven, J.D., Ackerson, K.L., English, M.R., Eather, R.H., and Carovillano, R.L.: "Global Auroral Imaging Instrumentation for the Dynamics Explorer Mission," Space Sci. Instr., vol. 5, p. 369, 1981.

Frank, L.A., Craven, J.D., Burch, J.L., and Winningham, J.D.: "Polar Views of the Earth's Aurora With Dynamics Explorer," Geophys. Res. Lett., vol. 9, p. 1001, 1982.

Fraser, G.W., and Pearson, J.F.: "Soft X-Ray Energy Resolution With Microchannel Plate Detectors of High Quantum Detection Efficiency," Nucl. Instr. Meth. in Phys. Res., vol. 219, p. 199, 1984.

Funsten, H.O., McComas, D.J., and Barraclough, B.L.: "Application of Thin Foils in Low Energy Neutral Atom Detection," SPIE, vol. 1744, p. 62, 1992.

Gladstone, G.R.: "Simulated Images of the Plasmasphere," SPIE, vol. 1744, p. 171, 1992.

Harris, W., Clarke, J., Caldwell, J.R., Bush, B., Cotton, D., Chakrabarti, S., and Feldman, P.: "A High Resolution UV Spectrograph for a Sounding Rocket Observation of the Jovian H Ly-α Profile," SPIE, vol. 1745, p. 251, 1992.

Herrero, F., and Smith, M.F.: "Imager of Low-Energy Neutral Atoms (ILENA): Imaging Neutrals From the Magnetosphere at Energies Below 20 keV," SPIE, vol. 1744, p.32, 1992.

Herrmann, M.C., and Johnson, C.L.: "Spacecraft Design Considerations for an Inner Magnetosphere Imager Mission," SPIE, vol. 1744, p. 2, 1992.

Hirao, K., and Itoh, T.: "Scientific Satellite Kyokko (Exos-A)," Solar Terr. Env. Res. in Japan, vol. 2, p. 148, 1978.

Hovestadt, D., and Scholer, M.: "Radiation Belt-Produced Energetic Hydrogen in Interplanetary Space," J. Geophys. Res., vol. 81, p. 5039, 1976.

Hsieh, K.C., and Curtis, C.C.: "Remote Sensing of Planetary Magnetospheres: Mass and Energy Analysis of Energetic Neutral Atoms, in Solar System Plasma Physics," eds. Burch, Waite, and Moore, vol. 159, AGU, Washington DC, 1989.

Huffman, R.E., LeBlanc, F.J., Larrabee, J.C., and Paulsen, D.E.: "Satellite Atmospheric Radiance Measurements in the Vacuum Ultraviolet," Tech. Rep. AFGL-TR-79-0151, Air Force Geophys. Lab., Bedford, Mass., 1979.

Huffman, R.E., LeBlanc, F.J., Larrabee, J.C., and Paulsen, D.E.: "Satellite Vacuum Ultraviolet Airglow and Auroral Observations," J. Geophys. Res., vol. 85, p. 2201, 1980.

Imhof, W.L., Nakano, G.H., Johnson, R.G., and Reagan, J.B.: "Satellite Observations of Bremsstrahlung From Widespread Energetic Electron Precipitation Events," J. Geophys. Res., vol. 79, p. 565, 1974.

Imhof, W.L., Voss, H.D., Datlowe, D.W., and Mobilia, J.: "Bremsstrahlung X-Ray Images of Isolated Electron Patches at High Latitudes," J. Geophys. Res., vol. 90, p. 6515, 1985.

Imhof, W.L., et al.: "The Polar Ionospheric X-Ray Imaging Experiment (PIXIE)," GGS Polar PI Instrument Manuel, 1991.

Imhof, W.L., Voss, H.D., and Datlowe, D.W.: "The Imaging of X-Rays for Magnetospheric Investigation," SPIE, vol. 1744, p. 196, 1992.

Ishimoto, M., Meng, C.-I., Romick, G.R., and Huffman, R.E.: "Doppler Shift of Auroral Lyman α Observed From a Satellite," Geophys. Res. Lett., vol. 16, p. 143, 1989.

Herrman, M.C., and Johnson, C.L.: "Spacecraft Design Consideration for an Inner Magnetosphere Imager Mission," SPIE, vol. 1744, p. 2, 1992.

Johnson, R.B.: "Wide Field of View Three-Mirror Telescopes Having a Common Optical Axis," Optical Eng., vol. 27, p. 1046, 1988.

Kearney, P.A., Slaughter, J.M., and Falco, C.M.: "Materials for Multilayer X-Ray Optics at Wavelengths Below 100 Å," Optical Eng., vol. 30, p. 1076, 1991.

Keath, E.P., Andrews, G.B., Cheng, A.F., Krimigis, S.M., Mauk, B.H., Mitchell, D.G., and Williams, D.J.: "Instrumentation for Energetic Neutral Atom Imaging of Magnetospheres," in Solar System Plasma Physics, eds. Burch, Waite, and Moore, vol. 165, AGU, Washington DC, 1989.

Kirsch, E., Krimigis, S.M., Kohl, J.W., and Keath, E.P.: "Upper Limits for X-Ray and Energetic Neutral Particle Emission From Jupiter: Voyager 1 Results," Geophys. Res. Lett., vol. 8, p. 169, 1981a.

Kirsch, E., Krimigis, S.M., Ip, W.H., and Gloeckler, G.: "X-Ray and Energetic Neutral Particle Emission From Saturn's Magnetosphere," Nature, vol. 292, p. 718, 1981b.

Krimigis, S.M., Kohl, J.W., and Armstrong, T.P.: "The Magnetospheric Contribution to the Quiet-Time Low-Energy Nucleon Spectrum in the Vicinity of the Earth," Geophys. Res. Lett., vol. 2, p. 457, 1975.

Kumar, S., Chakrabarti, S., Paresce, F., and Bowyer, S.: "The O^+ 834 Å Dayglow: Satellite Observations and Interpretation With a Radiation Transfer Model," J. Geophys. Res., vol. 88, p. 9271, 1983.

Lindblom, J.K., et al.: Multi-Spectral Solar Telescope Array IV: The Soft X-Ray and Extreme Ultraviolet Filters," Optical Eng., vol. 30, p. 1134, 1991.

Malherbe, A.: "Interference Filters for the Far Ultraviolet," Appl. Opt., vol. 13, p. 1276, 1974.

McComas, D.J., Funsten, H.O. III, Gosling, J.T., Moore, K.R., and Thomsen, M.F.: "Low-Energy Neutral-Atom Imaging," SPIE, vol. 1744, p. 40, 1992.

McEntire, R.W., and Mitchell, D.G.: "Instrumentation for Global Magnetospheric Imaging Via Energetic Neutral Atoms," in Solar System Plasma Physics, eds. Burch, Waite, and Moore, vol. 69, AGU, Washington DC, 1989.

McKenzie, D.L., Gorney, D.J., and Imhof, W.L.: "Auroral X-Ray Imaging From High- and Low-Earth Orbit," SPIE, vol. 1745, p. 39, 1992.

Meier, R.R., and Mange, P.: "Geocoronal Hydrogen: An Analysis of the Lyman-Alpha Airglow Observed From OGO-4," Planet. Space Sci., vol. 18, p. 803, 1970.

Mizera, P.F., Luhmann, J.G., Kolasinski, W.A., and Blake, J.B.: "Correlated Observations of Auroral Arcs, Electrons, and X-Rays From a DMSP Satellite," J. Geophys. Res., vol. 83, p. 5573, 1978.

Mizera, P.F., Gorney, D.J., and Roeder, J.L.: "Auroral X-Ray Images From DMSP-F6," Geophys. Res. Lett., vol. 11, p. 255, 1984.

Meier, R.R., and Weller, C.S.: "EUV Resonance Radiation From Helium Atoms and Ions in the Geocorona," J. Geophys. Res., vol. 77, p. 1190, 1972.

Meng, C.I., and Huffman, R.E.: "Ultraviolet Imaging From Space of the Aurora Under Full Sunlight," Geophys. Res. Lett., vol. 11, p. 315, 1984.

Ohashi, T., Makishima, K., Ishida, M., Tsuru, T., Tashiro, M., Mihara, T., Kohmura, Y., and Inoue, H.: "Imaging Gas Scintillation Proportional Counters for ASTRO-D, SPIE, vol. 1549, p. 9, 1991.

Orsini, S., et al.: "Proposal of an Italian Experiment for the Mission SAC-B. ISENA: Imaging Particle Spectrometer for Energetic Neutral Atoms," SPIE, vol. 1744, p. 91, 1992.

Paresce, F., Bowyer, C.S., and Kumar, S.: "On the Distribution of He^+ in the Plasmasphere From Observations of Resonantly Scattered He II 304 Å Radiation," J. Geophys. Res., vol. 79, p. 174, 1974.

Rairden, R.L., Frank, L.A., and Craven, J.D.: "Geocoronal Imaging With Dynamics Explorer," J. Geophys. Res., vol. 91, p. 13,613, 1986.

Rodgers, E.H., Nelson, D.F., and Savage, R.C.: "Auroral Photography From a Satellite," Science, vol. 183, p. 951, 1974.

Roelof, E.C., Mitchell, D.G., and Williams, D.J.: "Energetic Neutral Atoms (E ~ 50 keV) From the Ring Current: IMP 7/8 and ISEE 1," J. Geophys. Res., vol. 90, p. 10,991, 1985.

Roelof, E.C.: "Energetic Neutral Atom Images of a Storm-Time Ring Current," Geophys. Res. Lett., vol. 14, p. 652, 1987.

Schenkel, F.W., Ogorzalek, B.S., Gardner, R.R., Hutchins, R.A., Huffman, R.E., and Larrabee, J.C.: "Simultaneous Multispectral Narrow-Band Auroral Imagery From Space (1,150 to 6,300 Å)," in Ultraviolet Technology, SPIE, vol. 687, p. 90, 1986.

Schulze, D.W., Sandel, B.R., and Broadfoot, A.L.: "Multilayer Mirrors and Filters for Imaging the Earth's Inner Magnetosphere," SPIE, vol. 1549, p. 319, 1991.

Smith, B.W., Bloch, J.J., and Roussel-Dupré, D.: "Metal Multilayer Mirrors for the EUV/Ultrasoft X-Ray Wide-Field Telescopes," Optical Eng., vol. 29, p. 592, 1990.

Torr, D.G., Torr, M.R., Zukic, M., Spann, J., and Johnson, R.B.: "The Ultraviolet Imager (UVI) for ISTP," SPIE, vol. 1745, p. 61, 1992.

Viitanen, V.-P., Nenonen, S., and Sipilä, H.: "Soft X-Ray Windows for Position-Sensitive Proportional Counters," SPIE, vol. 1549, p. 28, 1991.

Voss, H.D., Mobilia, J., Collin, H.L., and Imhof, W.L.: "Satellite Observations and Instrumentation for Imaging Energetic Neutral Atoms," SPIE, vol. 1744, p. 79, 1992.

Weller, C.S., and Meier, R.R.: "First Satellite Observations of the He^+ 304 Å Radiation and Its Interpretation," J. Geophys. Res., vol. 79, p. 1572, 1974.

Wells, A., Castelli, C., Holland, A., McCarthy, K.J., Spragg, J.E., and Whitford, C.H.: "The CCD Focal Plane Imaging Detector for the JET-X Instrument on Spectrum R-G," SPIE, vol. 1549, p. 357, 1991.

Williams, D.J., Keppler, E., Fritz, T.A., Wilken, B., and Wibberenz, G.: "The ISEE 1 and 2 Medium Energy Particle Experiment," IEEE Trans. Geosci. Elec., GE-16, vol. 270, 1981.

Young, J.M., Weller, C.S., Johnson, C.Y., and Holmes, J.C.: "Rocket Observations of the Far UV Nightglow at Lyman α and Shorter Wavelengths," J. Geophys. Res., vol. 76, p. 3710, 1971a.

Young, J.M., Carruthers, G.R., Holmes, J.C., Johnson, C.Y., and Patterson, N.P.: "Detection of Lyman β and Helium Resonance Radiation in the Night Sky," Science, vol. 160, p. 990, 1971b.

Zukic, M., and Torr, D.G.: "High-Reflectivity Multilayers as Narrowband VUV Filters," SPIE, vol. 1485, p. 216, 1991.

Zukic, M., Torr, D.G., and Torr, M.R.: "High Throughput Narrowband 83.4 nm Self-Filtering Camera," SPIE, vol. 1549, p. 234, 1991.

Zukic, M., Torr, D.G., and Kim, J.: "Extreme Ultraviolet Filters for 58.4 and 83.4 nm," SPIE, vol. 1744, p. 178, 1992.

Zwick, H.H., and Shepherd, G.G.: "Some Observations of Hydrogen-Line Profiles in the Aurora," J. Atmospheric Terrest. Phys., vol. 25, p. 604, 1963.

REPORT DOCUMENTATION PAGE

Form Approved
OMB No. 0704-0188

Public reporting burden for this collection of information is estimated to average 1 hour per response, including the time for reviewing instructions, searching existing data sources, gathering and maintaining the data needed, and completing and reviewing the collection of information. Send comments regarding this burden estimate or any other aspect of this collection of information, including suggestions for reducing this burden, to Washington Headquarters Services, Directorate for information Operations and Reports, 1215 Jefferson Davis Highway, Suite 1204, Arlington, VA 22202-4302, and to the Office of Management and Budget, Paperwork Reduction Project (0704-0188), Washington, DC 20503

1. AGENCY USE ONLY *(Leave blank)*	2. REPORT DATE	3. REPORT TYPE AND DATES COVERED
	March 1993	Contractor Report (Final Report)

4. TITLE AND SUBTITLE
Inner Magnetosphere Imager (IMI) Instrument Heritage

5. FUNDING NUMBERS
G NGT-01-002-099

6. AUTHOR(S)
G.R. Wilson

7. PERFORMING ORGANIZATION NAME(S) AND ADDRESS(ES)
The University of Alabama in Huntsville
Huntsville, AL 35899

8. PERFORMING ORGANIZATION REPORT NUMBER
M-714

9. SPONSORING / MONITORING AGENCY NAME(S) AND ADDRESS(ES)
National Aeronautics and Space Administration
George C. Marshall Space Flight Center
Marshall Space Flight Center, AL 35812

10. SPONSORING / MONITORING AGENCY REPORT NUMBER
NASA CR-4498

11. SUPPLEMENTARY NOTES
This work was performed for the MSFC Program Development Directorate by Dr. Wilson as a part of the Summer Faculty Program

12a. DISTRIBUTION / AVAILABILITY STATEMENT
Unclassified — Unlimited
Subject Category: 46

12b. DISTRIBUTION CODE

13. ABSTRACT *(Maximum 200 words)*

This report documents the heritage of instrument concepts under consideration for the inner magnetosphere imager (IMI) mission. The proposed IMI will obtain the first simultaneous images of the component regions of the inner magnetosphere and will enable scientists to relate these global images to internal and external influences as well as local observations. To obtain simultaneous images of component regions of the inner magnetosphere, measurements will be made of:

- The ring current and inner plasma sheet using energetic neutral atoms
- The plasmasphere using extreme ultraviolet
- The electron and proton auroras using far ultraviolet and x rays
- The geocorona using FUV.

Instrument concepts that show heritage and traceability to those that will be required to meet the IMI measurement objectives are described.

14. SUBJECT TERMS
Inner Magnetosphere Imager (IMI), Magnetosphere, Aurora, Geocorona, Ultraviolet Imaging, Energetic Neutral Atom Imaging

15. NUMBER OF PAGES
32

16. PRICE CODE
A03

17. SECURITY CLASSIFICATION OF REPORT	18. SECURITY CLASSIFICATION OF THIS PAGE	19. SECURITY CLASSIFICATION OF ABSTRACT	20. LIMITATION OF ABSTRACT
Unclassified	Unclassified	Unclassified	Unlimited

NSN 7540-01-280-5500

Standard Form 298 (Rev 2-89)
Prescribed by ANSI Std Z39-18
298-102

NASA-Langley, 1993